CHALMERS
UNIVERSITY OF TECHNOLOGY

# Process Evaluation of Flue Gas Treatment for Pressurized Oxy-fuel Combustion Systems

Master's Thesis in the Master Degree Programme, Sustainable Energy Systems

Viktor Bood Rijal

Department of Space, Earth and Environmental Sciences
*Division of Energy Technology*
CHALMERS UNIVERSITY OF TECHNOLOGY
Göteborg, Sweden 2019

Master's thesis 2019

# Process Evaluation of Flue Gas Treatment for Pressurized Oxy-fuel Combustion Systems

VIKTOR BOOD RIJAL

Department of Space, Earth and Environmental Sciences
*Division of Energy Technology*
Chalmers University of Technology
Göteborg, Sweden 2019

Process Evaluation of Flue Gas Treatment for Pressurized Oxy-fuel Combustion Systems
VIKTOR BOOD RIJAL

Supervisors: Fredrik Normann and Sima Ajdari
Examiner: Fredrik Normann

Master's Thesis 2019
Department of Space, Earth and Environmental Sciences
Division of Energy Technology
Chalmers University of Technology
SE-412 96 Göteborg
Telephone +46 (0)31 772 1000

Göteborg, Sweden 2019

Process Evaluation of Flue Gas Treatment for Pressurized Oxy-fuel Combustion Systems
VIKTOR BOOD RIJAL
Department of Space, Earth and Environmental Sciences
Division of Energy Technology
Chalmers University of Technology

# Abstract

Pressurized oxy-fuel combustion with carbon capture allows for fossil fuel use with low greenhouse gas emissions. In order to avoid corrosion and emission of harmful species other impurities in the pressurized flue gas should be minimized. There is therefore an interest in the potential of simultaneous $NO_x$ and $SO_x$ removal by absorbtion into water under high pressure conditions. The treatment alternatives for the resulting liquid solution from such an absorption process is the main focus of this thesis.

The thesis compares the experimental work by Stanger et al. with the detailed reaction mechanism developed by Ajdari et al. through modelling [2], [1]. The model is validated by the experimental work and is thereafter used to evaluate the behaviour of the liquid, which was not measured during the experimental work.

The results show that releasing the liquid phase into a waste water pound would result in almost 40% of the nitrogen molecules being released as $N_2O$ to the air, which is not desired as $N_2O$ is a powerful greenhouse gas. It was also found that isolating the liquid phase would further increased the $N_2O$ formation.

The liquid phase also has a low pH value which needs to be taken into consideration. Over time it would decrease the pH value in the waste water pound. Lower pH value would also lead to increased $N_2O$ formation. Use of a buffer solution to keep the pH value in the waste water pound stable could be a potential solution.

Keywords: Pressurized oxy-fuel, flue gas, treatment, $NO_x$ and $SO_x$ chemistry

# Acknowledgements

Fredrik Normann for his guidance. The meetings and the feedback that you provided helped me a lot. Thank you for your time and effort, I am very grateful.

Thank you, Sima Ajdari, for the help in the early phase of the writing and especially in regards to the reaction mechanism and the work on the model.

Thank you, Shouzhuang Li, for being my opponent on short notice and for your good feedback on the thesis.

Viktor Bood Rijal, Gothenburg, April 2019

# Contents

# List of Figures

# List of Tables

# 1

# Introduction

## 1.1 Background

The emissions of greenhouse gases causing global warming is a major concern for today's society on a global level. The rise of greenhouse gas emissions is largely connected to the anthropogenic usage of fossil fuels. This concern has led to an increased debate over both greenhouse gas emissions and the usage of fossil fuels in society.

Oxy-fuel combustion is a method that enables the usage of fossil with low emissions of greenhouse gases. Oxygen is used instead of air as oxidant and the resultant flue gas stream gets a high concentration of carbon dioxide, which is suitable for carbon capture. There are, however, still impurities such as $NO_x$, $SO_x$ and water steam in the flue gas stream. These impurities need to be separated in as large extent as possible from the carbon dioxide before transportation and storage. Therefore the chemistry of the flue gas system is of high relevance to be able to separate as much as possible of the impurities while avoiding formation of more greenhouse gases, such as nitrous oxide, $N_2O$.

It is believed that oxy-fuel combustion under high pressure could be more effective than under atmospheric pressure which has previously been studied to a larger extent. The previous work has concluded that there is a need to quantify the impact that the mass transfer mechanism has on the system as well as the handling of the liquid waste stream that is generated in the system.

## 1.2 Objective

The focus areas of this work are illustrated in Figure 1.1 below. Through modelling with a detailed reaction mechanism by Ajdari et al. a comparison is made with the experimental work by Stanger et. al [1],[2]. The thesis therefore combine the work of these two groups.

To achieve the simultaneous $NO_x$ and $SO_x$ removal a liquid phase is added to the flue gases in a reactor. The main advantage of this process is that it would be a relatively cheap alternative for cleaning the flue gas from impurities without affecting the $CO_2$ as it does not require expensive material. This could make it a suitable combination with carbon capture to minimize emissions.

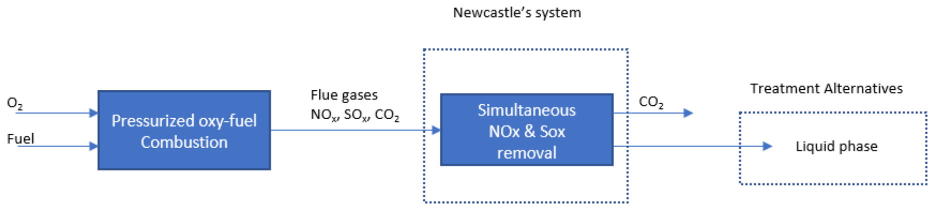

**Figure 1.1:** An overview of the system as a whole with the respective system boundaries shown for Newcastle's experiments and for the liquid phase whose treatment alternatives is studied.

The whole system from fuel to pressurized oxy-fuel combustion to the simultaneous $NO_x$ and $SO_x$ removal to the liquid phase and gas phase, which consists mainly of $CO_2$, is shown in Figure 1.1 above. The respective system boundaries that are taken into account for the model of the experiments performed at the University of Newcastle and for the treatment alternatives for the liquid phase are presented as well.

The main objective of this thesis though is to study how to treat the liquid phase that remains after the simultaneous $NO_x$ and $SO_x$ removal. As there is no data available on the liquid phase from the experimental work by Stanger et al, the data from the model based on their experiments is used as a basis for evaluating the treatment alternatives.

# 2

# Experimental work by Stanger et. al at the University of Newcastle

This chapter summarizes the experimental work performed by Stanger et. al at the University of Newcastle [2]. The focus of the work was to investigate the simultaneous $NO_x$ and $SO_x$ removal under high pressure conditions. This was done since this form of passive cleaning of the flue gases would lead to a reduction in cost as no additional equipment would be needed. It would also avoid absorption of $CO_2$ which is not desired if it is to be combined with carbon capture.

Particular focus was put on the potential formation of $N_2O$ which is a very powerful greenhouse gas. In order to investigate this they used two different experimental setups. Two different pressure levels were used in both the experimental setups, both a high pressure of 25 bar and a lower pressure of 5 bar.

## 2.1 Water vapour experiments

In these experiments liquid water was held in a reactor where $N_2$ carry gas was bubbled into the liquid water. The gas mixture was then mixed with 1000ppm $NO$, 1000ppm $SO_x$ while $O_2$ levels were constant at 5%. Three different parameters were varied between the experiments in the water vapour experimental setup. These parameters were residence time, presence of water vapour and the pressure.

In these experiments it was found that it was likely to be interaction between $SO_2$ and $NO_x$. The concentration of $SO_x$ and $NO_x$ decreased both with residence time and with pressure. The concentration of $N_2O$ in these experiments were at the lower detection limit for all conditions.

## 2.2 Continuous gas/batch liquid experiments

In the continuous gas/batch liquid experiments a gas flow was directed into the liquid in a reactor. The gas was allowed to contact the liquid for 4 hours before the flow was stopped and replaced with a flow of 5% $O_2$ and the remainder $N_2$. Two different pressure levels were used, a higher pressure level of 25 bar and a lower pressure level of 5 bar. At both pressure levels three different experiments were performed with different gas and liquid compositions. The different conditions for the experiments are presented in Table 2.1 below.

| Pressure | Gas composition | Liquid Composition |
|---|---|---|
| 5 bar | 5% $O_2$, 1000ppm $SO_x$, 1000ppm NO | Water |
| | 5% $O_2$, 1000ppm $SO_x$ | pH 1.5, $HNO_3$ |
| | 5% $O_2$, 1000ppm NO | pH 1, $H_2SO_4$ |
| 25 bar | 5% $O_2$, 1000ppm $SO_x$, 1000ppm NO | Water |
| | 5% $O_2$, 1000ppm $SO_x$ | pH 1.5, $HNO_3$ |
| | 5% $O_2$, 1000ppm NO | pH 1, $H_2SO_4$ |

**Table 2.1:** An overview over the settings used during the experiments at the University of Newcastle.

In the first experimental setup, when there was $SO_x$ and $NO_x$ in the gas flow that enter a liquid phase that consisted of water it was seen that both increased pressure and increased residence time increased the interaction between $SO_x$ and $NO_x$.

At 5 bar there was $N_2O$ formation throughout the whole experiment, while at 25 bar the $N_2O$ formation stopped after the initial formation and only started again for the final minutes of the experiment. The initial formation peaked at 100ppm in the 25 bar experiment. Overall much less $N_2O$ was formed in the 25 bar experiment than in the 5 bar experiment. This was despite a higher absorption rate of both $SO_x$ and $NO_x$ at 25 bar.

In the second experimental setup for the continuous gas/batch liquid experiments $SO_x$ entered with the gas flow into a liquid phase consisting of $HNO_3$. In this setup there was an initial, but brief, $NO_2$ formation at 5 bar, while there was $N_2O$ formation for approximately two hours at 25 bar. As the absorption of $SO_x$ decreased over time the formation of $N_2O$ decreased and eventually reached zero. The formation of $N_2O$ was greater at 25 bar pressure than at 5 bar.

For the third experimental setup where $NO_x$ entered with the gas flow into a liquid phase consisting of $H_2SO_4$ there was no formation of $N_2O$. Without the absorption of $SO_2$ that occurred in the previous experiments there was no $HSO_3^-$ formation. The $HSO_3^- -$ is necessary for $N_2O$ formation.

## 2.3 Summary

The experiment that is of the most relevance for this thesis is the experiment at a pressure of 25 bar where both $SO_x$ and $NO_x$ enter with the gas flow and bubble through the liquid phase that consists of water. An approximation of the result of this experiment is shown in Figure 2.1 below

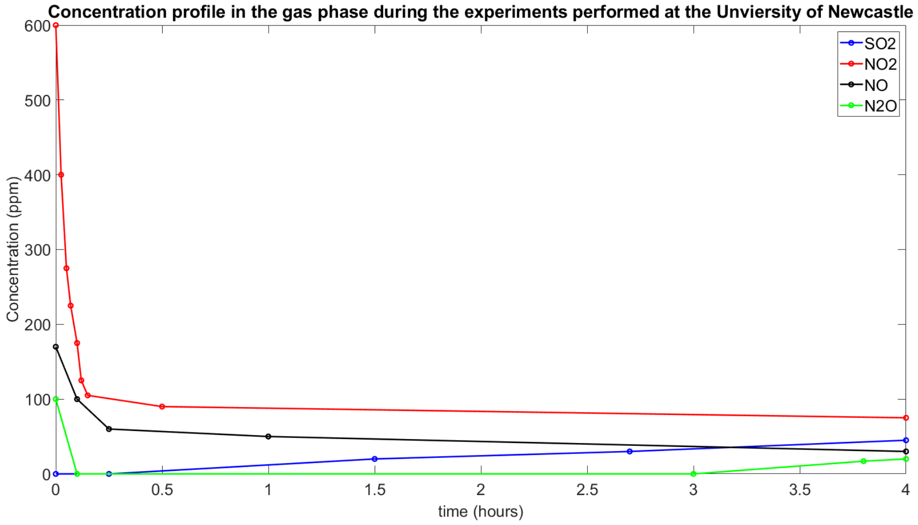

**Figure 2.1:** A summary over the concentration in the gas phase at the outlet of the reactor in the continuous gas/batch liquid experiment at a pressure of 25 bar with both $NO_x$ and $SO_x$ present in the gas phase and water in the liquid phase.

In the graph it can be seen that initially all $SO_2$ gets absorbed and then the amount at the outlet increases over time to almost 50ppm at the outlet at the end of the experiment. There is about 100ppm $NO_2$ at the outlet of the reactor at the beginning of the experiment and it decreases slightly over time. The NO, similarly, is at approximately 50ppm at the beginning of the experiment and decreases over time. There is some initial $N_2O$ formation at the beginning of the experiment and after that there is no formation until the last 1.5 hours, where there is a low amount of $N_2O$ formation.

In their experiment they also included a dry $NO_x/SO_x$ interaction, where the gases were allowed to interact with each other for 30 minutes, without the presence of the liquid phase. This was not included in Figure 2.1 above. During their dry interaction the $SO_2$ decreased from 1000ppm to just below 500ppm, while $NO_2$ went up to almost 600ppm and NO to about 100ppm. They believe the explanation to this is that there was interaction between $SO_2$ and $NO_x$ in the gas phase.

The overall conclusions that they draw from these experiments and the comparisons they made with literature is that $N_2O$ can only be formed when the liquid phase contains both $HNO_2$ and $HSO_3^-$. This condition was only satisfied in the experiments where either both $NO_x$ and $SO_x$ entered with the gas flow into a liquid phase consisting of water or where $SO_x$ entered with the gas flow into a liquid phase already consisting of $HNO_3$. This was true for their experiments even though pH levels were above 2, which is inconsistent with other findings.

# 3

# Theory

This chapter will go through the theory that is relevant for the system and the model.

## 3.1 Reaction chemistry for the $NO_x/SO_x$ reactor

After a pressurized oxy-fuel combustion with a carbon based fuel the flue gas composition consists of mainly carbon dioxide, to about 95%. There is also some inert nitrogen (2%) which remains after the combustion as well as $SO_x$, $NO_x$ , water vapour and oxygen.

The reaction chemistry section goes over the reactions that are considered to be of importance in the system. There are relevant reactions occurring in both the gas phase and the liquid phase of the system. Most of the reactions that are considered are in the liquid phase where they are grouped as $NO_x$ reactions, $SO_x$ reactions, N-S reactions and carbon reactions. The name of the group tells which group of molecules that are involved in the reactions, where N-S reactions are reactions that include both $NO_x$ and $SO_x$. The reaction chemistry is based on the detailed reaction mechanism developed by Ajdari et al. [1].

It is important to consider all of these groups of reactions since they affect each other and the reaction chemistry plays an important role for the concentrations at the outlet of the system. The importance of the reactions can vary with temperature, pressure and pH.

### 3.1.1 Reaction chemistry in the gas phase

The most important reaction in the gas phase is the oxidation of nitric oxide (NO) to nitrogen dioxide ($NO_2$). The rate of this reaction heavily depends on the pressure of the system and increases with increasing pressure. It is also of importance to the system that the nitrogen dioxide has a considerably higher solubility in water than the nitric oxide, to about a magnitude of ten. The reaction can be seen in reaction 3.1 below

$$2NO + 2O_2 \longrightarrow 2NO_2 \tag{3.1}$$

The other relevant reactions in the gas phase are the reactions between two nitrogen dioxide molecules to form dinitrogen tetroxide ($N_2O_4$) and the reaction between nitric oxide, nitrogen dioxide and water vapour to form nitrous acid ($HNO_2$) as can be seen in reaction 3.2 and 3.3 below

$$\mathrm{NO_2} + \mathrm{2O_2} \longrightarrow \mathrm{N_2O_4} \tag{3.2}$$

$$\mathrm{NO} + \mathrm{NO_2} + \mathrm{H_2O} \longrightarrow \mathrm{2HNO_2} \tag{3.3}$$

### 3.1.2 $\mathrm{NO}_x$ reaction chemistry in the liquid phase

It is mainly $\mathrm{NO_2}$ and $\mathrm{N_2O_4}$ entering the liquid phase through mass transfer from the gas phase. Then there is a variation of different reactions that are relevant to consider in the liquid phase for the $\mathrm{NO}_x$ groups. The new products include $\mathrm{HNO_2}$, $\mathrm{HNO_3}$, $\mathrm{N_2O_4}$, $\mathrm{NO_2^-}$ and $\mathrm{NO_3^-}$. These reactions can be seen below in reaction 3.4-3.9.

$$\mathrm{HNO_2} \longrightarrow \mathrm{NO_2^-} + \mathrm{H^+} \tag{3.4}$$

$$\mathrm{HNO_3} \longrightarrow \mathrm{NO_3^-} + \mathrm{H^+} \tag{3.5}$$

$$\mathrm{2NO_2} + \mathrm{H_2O} \longrightarrow \mathrm{HNO_2} + \mathrm{HNO_3} \tag{3.6}$$

$$\mathrm{2NO_2} \longrightarrow \mathrm{N_2O_4} \tag{3.7}$$

$$\mathrm{2HNO_2} \longrightarrow \mathrm{NO} + \mathrm{NO_2} + \mathrm{H_2O} \tag{3.8}$$

$$\mathrm{N_2O_4} + \mathrm{H_2O} \longrightarrow \mathrm{HNO_2} + \mathrm{HNO_3} \tag{3.9}$$

### 3.1.3 $\mathrm{SO}_x$ reaction chemistry in the liquid phase

The main $\mathrm{SO}_x$ component entering the liquid phase through mass transfer from the gas phase is $\mathrm{SO_2}$. The products from the $\mathrm{SO}_x$ reaction chemistry are $\mathrm{SO_4^{2-}}$, $\mathrm{SO_3^{2-}}$, $\mathrm{HSO_3^-}$ and $\mathrm{HSO_4^-}$ which can be viewed in reaction 3.10-3.13 below.

$$\mathrm{HSO_4^-} \longrightarrow \mathrm{SO_4^{2-}} + \mathrm{H^+} \tag{3.10}$$

$$SO_2 + H_2O \longrightarrow HSO_3^- + H^+ \tag{3.11}$$

$$HSO_3^- \longrightarrow H^+ + SO_3^{2-} \tag{3.12}$$

$$H_2SO_4 \longrightarrow HSO_4^- + H^+ \tag{3.13}$$

### 3.1.4 Nitrogen and sulphur reaction chemistry in the liquid phase

There are also reactions where nitrogen components and sulphur components react with each other. The most important reactions of these are shown in reaction 3.14-3.17 below. Where NSS stands for nitrososulfonic acid, $ONSO_3^-$, and HADS stands for hydroxylamine disulfonic acid, $HON(SO_3)_2^{2-}$.

$$HNO_2 + HSO_3^- \longrightarrow NSS + H_2O \tag{3.14}$$

$$NSS + HSO_3^- \longrightarrow HADS \tag{3.15}$$

$$NSS + \tfrac{1}{2}H_2O \longrightarrow N_2O + HSO_4^- \tag{3.16}$$

$$2NO_2 + SIV + H_2O \longrightarrow HSO_4^- + HNO_2 \tag{3.17}$$

## 3.2 Mass transfer

Mass-transfer operations such as gas absorption involves a solute being transferred from the gas phase into the liquid phase. The transfer at the interface then involves transfer of mass from the bulk of the gas phase into the interfacial surface, the transfer through the interface into the liquid phase and the transfer to the bulk of the liquid phase. This type of operation is often described with the two-resistance theory. The two resistance theory works under the principal assumption that the mass transfer between the two phases is controlled by the rates of diffusion through the phases on each side of the interface. It also assumed that there is no resistance to the mass transfer through the interface. The rate of diffusion can be described with

$$J_A = k_G(p_{A,L} - p_{A,i}) \tag{3.18}$$

for the gas phase and with

$$J_A = k_L(C_{A,i} - C_{A,L}) \tag{3.19}$$

for the liquid phase. Where $J_A$ is the rate of diffusion, $k_G$ is the convective mass transfer coefficient on the gas side, $k_L$ is the convective mass-transfer coefficient in the liquid phase, $p_{A,g}$-$p_{A,I}$ is the partial pressure difference and driving force for the mass transfer in the gas phase and $C_{A,i}$-$C_{A,L}$ is the concentration difference and driving force for the mass transfer in the liquid phase [3]. Calderbank and Moo-Young recommend the following correlations for the convective mass-transfer coefficient in the liquid phase when the bubble diameter, $d_b$, is smaller than 2.5 mm

$$k_L = 0.31D_{AB}^{2/3}(\frac{\rho_L g}{\mu_L})^{1/3} \tag{3.20}$$

and when the bubble diameter, $d_b$, is larger than 2.5 mm they recommend the following correlation

$$k_L = 0.42D_{AB}^{1/2}(\frac{\rho_L^{1/2} g}{\mu_L^{1/2}})^{1/3} \tag{3.21}$$

The mass transfer, $J_A$, can also be described by the overall mass transfer coefficient, $K_L$ for the liquid side based overall mass transfer coefficient. The liquid side based correlation is then written with the concentration where it is at an equilibrium at the film, $C_A^*$, and the concentration in the liquid bulk, $C_{A,L}$.

$$J_A = K_L(C_A^* - C_{A,L}) \tag{3.22}$$

$C_A^*$ can be calculated as the partial pressure divided by Henry's coefficient at low values of Henry's coefficient [3].

### 3.2.1 Diffusion coefficient

The diffusion coefficient, $D_{AB}$, for the liquid phase is described by the correlation proposed by Wilke and Chang in equation 3.23 below.

$$D_{AB} = \frac{7.4 \cdot 10^{-8} T(\Phi_B M_B)^{1/2}}{V_A^{0.6}\mu_B} \tag{3.23}$$

Where A is the molecule diffusing through the liquid solvent B. The solvent is assumed to be water for all the liquid side diffusion since most of the liquid is water. $\Phi_B$ is an association parameter, $M_B$ is the molecular weight, $\mu_B$ is the viscosity and $V_A$ is the molal volume of molecule A [3]. The diffusion coefficient is then calculated for all the respective molecules that are accounted for in the liquid phase.

The diffusion coefficients in the gas phase is approximated as binary diffusion of molecule A through molecule B. The diffusivities are calculated by Fuller, Schettler and Giddings' empirical equation as

$$D_{AB} = \frac{0.00143T^{1.75}}{P \cdot M_{AB}^{1/2}((\sum V)_A^{1/3} + (\sum V)_B^{1/3})^2} \tag{3.24}$$

The sum of V is the sum of the atomic and structural diffusion volumes relevant to the respective molecules in the diffusion, P is the pressure, T is the temperature while $M_{AB}$ is calculated as shown in equation 3.25

$$M_{AB} = \frac{2}{\frac{1}{M_A} + \frac{1}{M_B}} \tag{3.25}$$

Where $M_A$ is the molecular weight of the molecule that is diffusing through and $M_B$ is the molecular weight of the molecule that is being diffused through.

## 3.3 Bubble Columns

The upwards flow of gas bubbles in bubble columns appear in three different flow regimes. These flow regimes are the homogeneous flow regime, the heterogeneous flow regime and the slug flow regime. The main factor that decides which regime that will be applied in a bubble column is the superficial velocity of the gas. The different flow regimes have different implications on other relevant factors such as hydrodynamics, pressure drop, hold up of different phases, fluid-fluid interfacial areas, and interphase mass and heat transfer coefficients.

At low superficial gas velocities from 0.03 m/s to 0.08 m/s the homogeneous flow regime appears. The homogeneous flow regime has a narrow bubble-size distribution and the bubbles are distributed relatively uniformly over the reactor's cross-section. At higher superficial gas velocities the heterogeneous flow regime occurs. At this regime large bubbles with high rise velocities appear together with smaller bubbles. The large bubbles can have bubble diameters of up to 0.15 meters.

For high superficial gas velocities in reactors with small diameters slug flow can occur. The large bubbles are then stabilized by the reactor walls, which leads to formation of bubble slugs. These bubble slugs can occur in reactors with diameters up to 0.15 meters [6].

Gas holdup, bubble diameter and the interfacial surface area between the two phases are linked as can be seen in equation 3.26 and 3.27.

$$a = \frac{6H}{D_{BM}} \tag{3.26}$$

Where a is the interfacial surface area, H is the gas holdup and $D_{BM}$ is the average diameter of the bubbles in the column [5]. The gas holdup is defined as the volume of the gas phase divided with the total volume of the dispersion [6].

$$H = \frac{V_G}{V_G + V_L} \tag{3.27}$$

Where $V_G$ is the volume of the gas phase and $V_L$ is the volume of the liquid phase.

# 4

# Methods

This chapter describes the methodology used in this thesis. An overview picture of the steps involved in the method can be seen in Figure 4.1 below.

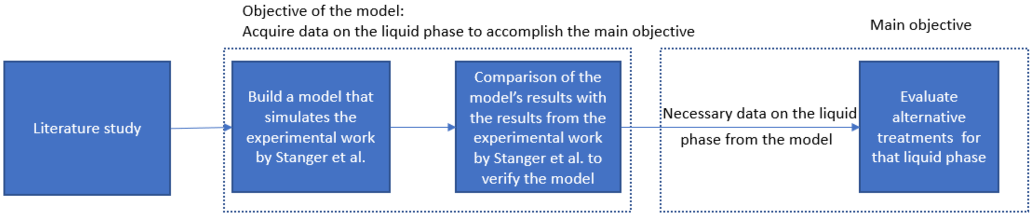

**Figure 4.1:** A flowchart over the steps involved in the work of this thesis and as such an overview over the method.

As the main objective of the thesis is to evaluate the treatment alternatives of the liquid phase that remains after the reactor for simultaneous $NO_x$ and $SO_x$ removal it was necessary to have data on the composition of the liquid phase. The experimental work by Stanger et al. did not have this data and therefore it was important to build a model to simulate the experiments that were performed and acquire the data on the liquid phase from the model instead.

The experimental work by Stanger et al. was still crucial to the thesis as they could be used as a basis for the model and to verify that the results from the model are reasonable.

The first step of the thesis was to perform a literature study on the necessary theory to both create the model and to be able to make the evaluation of the treatment alternatives for the liquid phase. Both the detailed reaction mechanism developed by Ajdari et al. and the experimental work by Stanger et al. were part of the initial literature study.

The model was built with the objective of simulating the experimental work by Stanger et al. in order to acquire data on the remaining liquid phase from the reactor for the simultaneous $NO_x$ and $SO_x$ removal. The gas phase composition that was obtained from the model was compared with the gas phase composition that was measured during the experimental work by Stanger et al. in order to verify the results from the model. The model uses the detailed reaction mechanism developed by Ajdari et al.

After verifying the results from the model the composition of the remaining liquid phase was used as a basis on which the different treatment alternatives for the liquid phase were evaluated, which also was the main objective to achieve for the thesis as a whole.

The evaluated treatment alternatives for the liquid phase:

- Keeping the liquid phase isolated.
- Release of the liquid phase into a waste water pound.
- Release of the liquid phase into a waste water pound after having kept it isolated.

# 5

# Model

The model was constructed to simulate the experimental work by Stanger et al. Their experiments were on simultaneous $NO_x$ and $SO_x$ removal from the flue gases after a pressurized oxy-fuel combustion. The model describes both the flue gas composition, its reaction chemistry, mass transfer and the reactor itself.

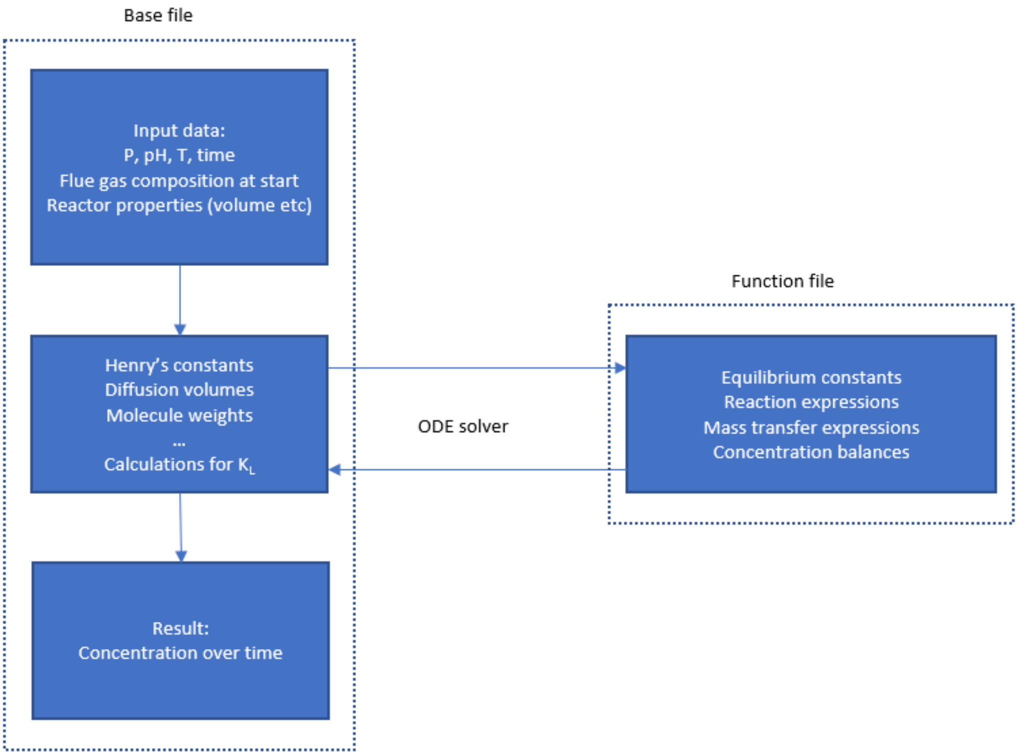

**Figure 5.1:** A basic schematic over how the model's files function in MATLAB.

The model is developed in MATLAB and a basic overview over how it functions can be viewed in Figure 5.1 above. Where the base file contains the basic information of the system, such as pressure, pH, temperature, time and the composition of the gas phase at the start. It also contains the necessary calculations for the mass transfer coefficients for this system. While the function file contains the equilibrium constants, the reaction expressions, the mass transfer expressions and the concentration balances that are solved with an ordinary differential equation solver to give how the composition of the gas and liquid phase changes over time.

The reactor is assumed to function as a bubble column, where there is gas in the head of the column and a liquid phase, consisting of water, below and then the flue gases bubbles up from the bottom of the column. This means that the gas phase has a residence time, which is the time it takes the gas phase to travel from the bottom and then to bubble all the way through until it exits at the top. There is a continuous flow of gas phase entering the reactor, while the liquid phase remains in the reactor throughout the whole experiment. The pressure in the is at 25 bar in the reactor and the dimensions of the reactor are based on the data from the experimental work by Stanger et al. as is the composition of the flue gases that bubble through the reactor which can be seen in the table below. In reality after a pressurized oxy-fuel combustion there would also be $CO_2$ in the flue gases. It is however a reasonable simplification to exclude the $CO_2$ since it would be mostly inert and therefore remain in the gas phase throughout. The focus is on how much of the other impurities that can be removed from the gas phase so that carbon capture efficiently can be applied at a later stage. The general system and reactor information such as pressure, volumes, flow rate and composition are presented in Table 5.1 below.

| System information | |
|---|---|
| Pressure | 25 bar |
| Gas composition | 5% $O_2$, 1000ppm $SO_x$, 1000ppm NO |
| Liquid Composition | Water |
| Reactor Volume | 300 mL |
| Liquid Volume | 150 mL |
| Gas flowrate | 2 SLPM |
| Gas residence time | 151 s |

**Table 5.1:** An overview over some of the general system information for the reactor in the model at the start of the simulations.

The gas phase in the system is described as a plug flow reactor (PFR), which is approximated as a series of continually stirred tank reactors (CSTR). When the number of CSTRs in a series is large enough they can be assumed to well describe the behavior of a PFR [7]. This is achieved in the model by dividing the total reactor volume into a number of equally sized CSTRs with equal residence times.

Concentration balances are then set up as a set of coupled differential equations, with one equation for every species involved, which are solved with an ordinary differential equation (ODE) solver for every CSTR. The calculated outlet concentration from reactor j is then set to be the inlet concentration to reactor j+1. The concentration balances for the gas phase include the reactions in the gas phase and the mass transfer to and from the liquid phase as is shown in the equation below. The concentration for the gas phase is written on the basis of partial pressure which makes the unit bar per second for the balances.

$$\frac{dp_i}{dt} = \sum RT(v_{i,j}R_{j,g}) - J_i \tag{5.1}$$

Where $v_{i,j}$ is the stoichiometric coefficient of species i in reaction j, $R_{j,g}$ is the rate of the reaction j in the gas phase, $J_i$ is the rate of mass transfer for species i and $p_i$ is the partial pressure of species i.

The liquid phase is described as a batch reactor since it remains in the reactor throughout the whole experiment with no flow neither in or out. While the gas phase is described with a series of CSTRs the liquid phase is described as a single batch reactor. There is a balance between each CSTR and the batch reactor and there is mass transfer between them. The concentration balance on the liquid side is described as shown in the equation below

$$\frac{dC_i}{dt} = \sum (v_{i,j} R_j) + J_i \frac{V_g}{V_l} \tag{5.2}$$

Where $v_{i,j}$ is the stoichiometric coefficient of species i in reaction j, $R_{j,l}$ is the rate of the reaction j in the liquid phase, $J_i$ is the rate of mass transfer for species i and $C_i$ is the concentration of species i. $(V_g/V_l)$ is the ratio of the volume of the gas phase to the volume of the liquid phase.

The balances in Equation 5.1 and 5.2 for the gas phase and liquid phase are solved simultaneously by using a solver for ordinary differential equations. The ordinary differential equation solver is used once for every CSTR's concentration balance for the gas phase together with the entire batch reactor's concentration balance for the liquid phase. The concentration at the outlet of a reactor couple is set to be the inlet concentrations to the following couple. There is a continuous flow of gas which enters the reactor with the same inlet concentration, while the liquid remains in the batch reactor throughout the duration. A basic schematic over how these reactors function in the model can be seen in Figure 5.2 below.

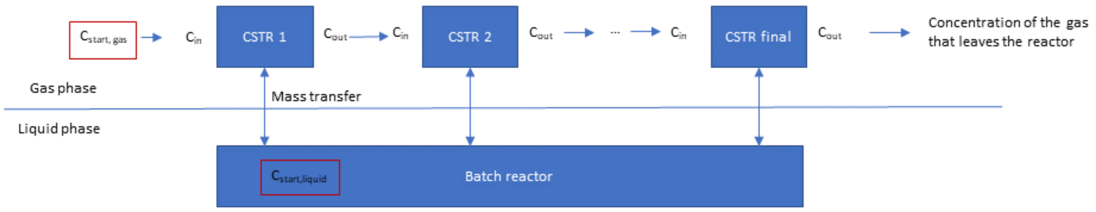

**Figure 5.2:** A basic schematic over how the series of reactors function in the model.

The model is validated by comparing the composition of the gas phase in the model with the measured results from the experiments performed at the University of Newcastle. It is worthwhile to note that it is the final $C_{out}$ values over time that are compared with the measured gas phase composition in the experimental work by Stanger et al.

The final gas phase composition changes over time, despite constantly having the same concentration when it begins to bubble through the reactor. This happens since the liquid phase remains in the reactor throughout the whole experiment and its composition changes over time as mass transfer between the phases and reactions occur. While it is the liquid phase's composition that is the most interesting for the main objective of this thesis, the evaluation of treatment alternatives for this liquid phase.

## 5.1 Evaluation of treatments for the liquid phase

The liquid phase for which different treatment alternatives were evaluated is the liquid phase that remains in the reactor for the simultaneous $NO_x$ and $SO_x$ removal. The different treatment alternatives are described and evaluated using MATLAB and the important mechanisms for each of the alternative treatments are taken into consideration, such as the relevant reaction kinetics and the mass transfer mechanism.

The first alternative to evaluate is to isolate the liquid phase and to study how the composition is affected. This is done both by keeping the liquid phase at 25 bar as well as lowering the pressure to 1 atmosphere. This is not only done for the purpose of storing the liquid as that may not be necessary, but also to see whether it is advantageous to keep it isolated before using another treatment.

The second treatment that is evaluated is to let the liquid phase enter a larger body of water, a waste water pound. This will be studied both by releasing the liquid phase immediately after the $NO_x/SO_x$ reactor as well as after the the liquid phase has held isolated in the previous alternative.

These simulations will be performed using a modified version of the model made for the reactor with simultaneous $NOx$ and $SO_x$ since the components and the relevant reactions are the same. The pH level will be kept constant in each simulation as an approximation since the volume of a waste water pound is large and would cause pH changes to be slow. Instead the simulations will be made at lowering pH levels as the pH would still be likely to drop over time if there was a continuous release of the liquid phase.

### 5.1.1 Isolation

The treatment alternative that is studied first is what happens if the liquid phase is kept isolated. The key characteristics for this is that there is no gas phase present which also means that there is no possibility of mass transfer between phases. The pressure has no direct impact on the liquid phase in the model and is therefore not important in this scenario.

### 5.1.2 The waste water pound

In the second alternative treatment the liquid phase is released into a waste water pound. This treatment will be evaluated both when the liquid phase is released directly into the waste water pound after the reactor for simultaneous $NO_x$ and $SO_x$ removal as well as when the liquid phase has first been kept isolated.

It is important to note that in the scenario of releasing the liquid into a waste water pound there will be mass transfer between the liquid phase and the gas phase, but the contact area between the phases is not as good as it was in the reactor for simultaneous $NO_x$ and $SO_x$ removal. The gas phase is approximated as only nitrogen and oxygen, while the waste water pound is approximated as pure water and the simulations are done at atmospheric pressure. The volume of the gas phase is assumed to be much larger than the volume of the waste water pound.

# 6

# Results and discussion

## 6.1 Parameter fitting and model validation

The simulations of the experimental work by Stanger et al. are done at the higher pressure level, 25 bar, as that is the focus of this thesis.

The result of the simulation of the experiment with 5% $O_2$, 1000ppm $SO_x$ and 1000ppm $NO_x$ can be viewed in Figure 6.1 below. It is important to note that the graph shows the gas composition only at the very end of the reactor and its changes at that point over time. The formation of $N_2O$ is low throughout the 4.5hrs long simulation, which is the same duration as for the experimental work by Stanger et al. The amount of $NO$ and $NO_2$ present at the exit of the reactor is constant at a low level through the entire simulation. Similarly the level of $SO_2$ is essentially zero throughout the simulation. The volume of the liquid phase in the reactor is sufficient to be able to efficiently absorb the $SO_2$ that enters with the gas.

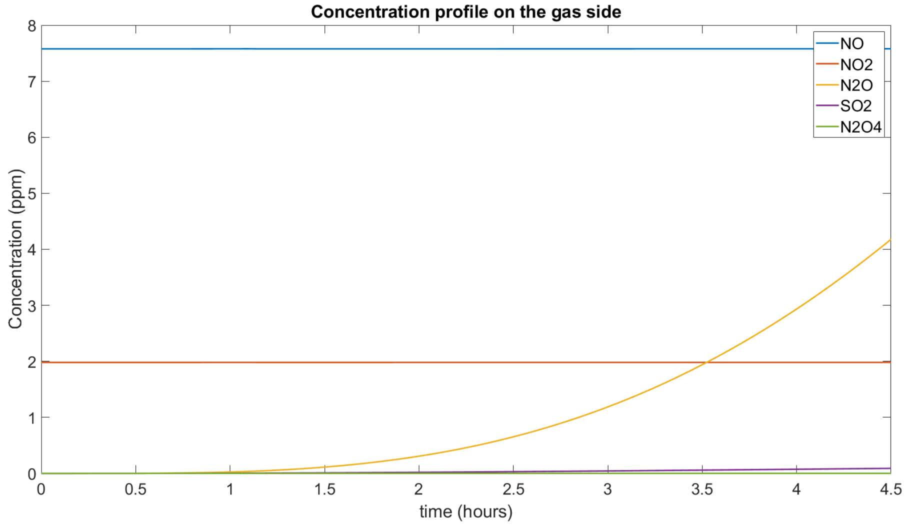

**Figure 6.1:** The concentration profile over the gas phase in the simulation of the experiment at the University of Newcastle.

The trend in the formation of $N_2O$ in the simulation is similar to the one in the experimental work by Stanger et al., but at a lower level. The absorption of both $NO_x$ and $SO_x$ is very efficient in the simulations, more efficient than in the experimental work. It should also be noted that the pH level drops to approximately 3.5

at the end from 7 where it is at the beginning of the simulation.

### 6.1.1 Sensitivity Analysis of the $SO_2$ absorption

In a system where $SO_2$ is absorbed into water it is expected that the water can only absorb a certain amount of $SO_2$ before being completely saturated. In regards to figure 6.1 above that would mean that after enough time the $SO_2$ would start increasing until it reached the same amount as it had at the inlet, 1000ppm. This would happen since no further absorption of $SO_2$ would be possible at that point.

However, in this case the time was not extended, but instead the volume of liquid was decreased. Decreasing the volume is another way to test the same phenomena as the volume of the liquid impacts how much $SO_2$ that is possible to absorb.

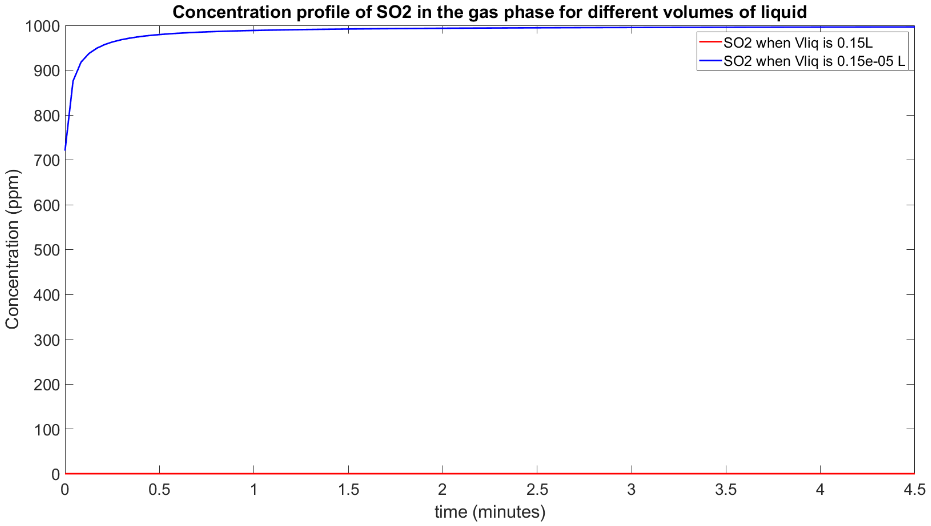

**Figure 6.2:** The concentration profile over the $SO_2$ in the gas phase at the outlet of the reactor compared to different volumes on the liquid phase.

As can be seen in Figure 6.2 above the amount of $SO_2$ at the outlet of the reactor increases as the volume of the liquid decreases, this means that as the volume of the liquid decreases it is not able to absorb as much $SO_2$. The first case in the figure is the with the same settings as in the original simulation, while the other case is with a much smaller volume of the liquid. This shows that if the volume of liquid is small enough or similarly the time of the simulation is long enough the liquid will become fully saturated of $SO_2$ and unable to absorb more. At that point all $SO_2$ that enters with the gas at the inlet will also leave with the gas at the outlet.

This also shows that there is a discrepancy between the model and the results from the experimental work by Stanger et al. as the absorption of $SO_2$ decreases over time there, but not in the model.

### 6.1.2 Sensitivity analysis of the mass transfer coefficient

Since the level of $SO_x$ and $NO_x$ at the outlet of the reactor in the simulation were lower than at the outlet during the experimental work by Stanger et al. that could imply that the absorption in the model is too efficient. Therefore a sensitivity analysis is performed on the mass transfer coefficients that are used. This is done by dividing the mass transfer coefficients that was calculated in the original model and evaluating the impact it has on the composition of the gas phase at the outlet of the reactor. The comparison can be seen in Figure 6.3 below.

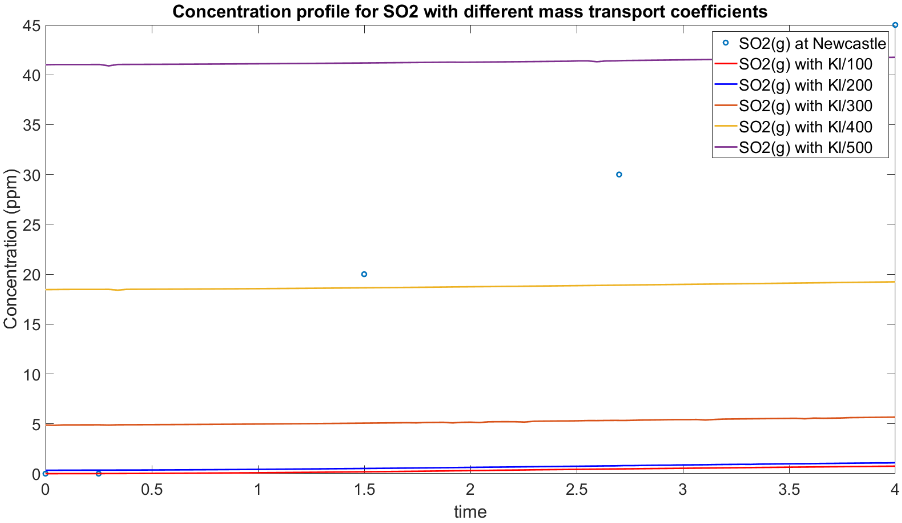

**Figure 6.3:** Comparison of the $SO_2$ absorption for different mass transfer coefficients.

Decreasing the mass transfer coefficient does increase the amount of $SO_2$ that remains in the gas phase and the case with Kl/500 has a similar amount at the end of the experiment. However, in the experimental work by Stanger et al. the $SO_2$ has a steady growth throughout the experiment while the concentration through the simulations in the model is very stable. This implies that the mass transfer coefficient indeed does affect the level of absorption of $SO_2$, but it is not able to give a similar trend as in the experimental work by Stanger et al.

### 6.1.3 Adapting the model to fit with the results of the experimental work

The main objective of the thesis is to analysis treatment alternatives for the liquid phase that remains after the simultaneous $NO_s$ and $SO_x$ removal of the flue gases. Therefore it is interesting to fit the model to the results that were achieved during the experimental work by Stanger et al.

From the sensitivity analysis above it can be seen that changing the mass transfer coefficient does not improve the results of the model. The $SO_2$ absorption in the results from the experimental work by Stanger et al. was very low at the beginning of the experiment and decreasing the mass transfer coefficient, while getting more similar $SO_2$ levels at the end of the simulation, counteracts that. Dividing the mass transfer coefficient by 200 brings up the level of $SO_2$ at the beginning of the simulation though, which makes it a better fit to the experimental results.

It can be seen during the sensitivity analysis of the volume of the liquid that decreasing that leads to an increased $SO_2$ absorption over time, similar to the one from the experimental work. Therefore it is of interest to study how well the results from the model with different volumes of liquid can fit the results of the experimental work by Stanger et al. while the volume of the gas phase was not changed. The results of this be seen in Figure 6.4 below.

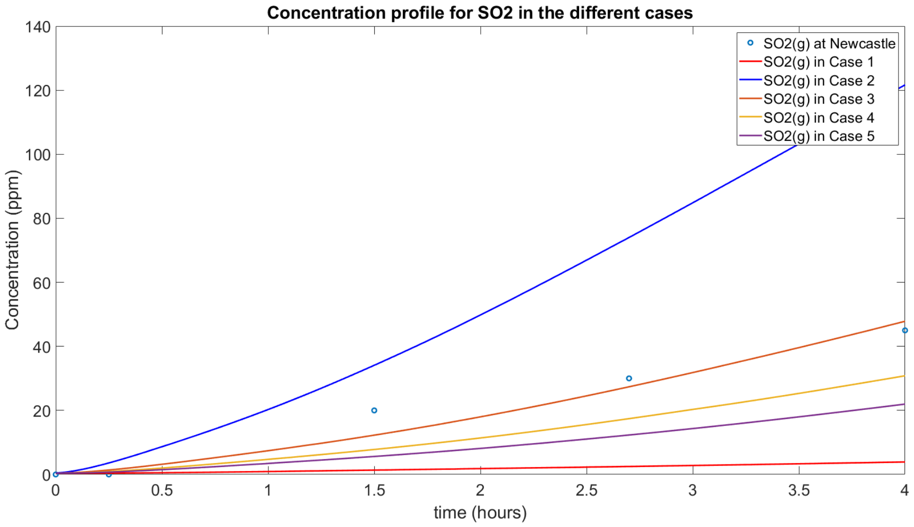

**Figure 6.4:** Fitting of the model to the results of the experiments performed at the University of Newcastle in regards to $SO_2$ absorption. I) Case 1: $V_{liq}/V_{gas} = 0.33$, II) Case 2: $V_{liq}/V_{gas} = 0.03$, III) Case 3: $V_{liq}/V_{gas} = 0.07$, IV) Case 4: $V_{liq}/V_{gas} = 0.09$, V) Case 5: $V_{liq}/V_{gas} = 0.11$.

The mass transfer coefficients were divided by 200 for all the cases. When the volume of the liquid phase was decreased to 0.003 L which corresponded to a volume ratio, $V_{liq}/V_{gas}$, of 0.07 it fit well with the $SO_2$ absorption achieved in experimental work. This is case 3 in Figure 6.4 above. The results from using these values of the mass transfer coefficients and the volume of the liquid in the model in comparison with the results of the experimental work by Stanger et al. can be seen in Figure 6.5 below.

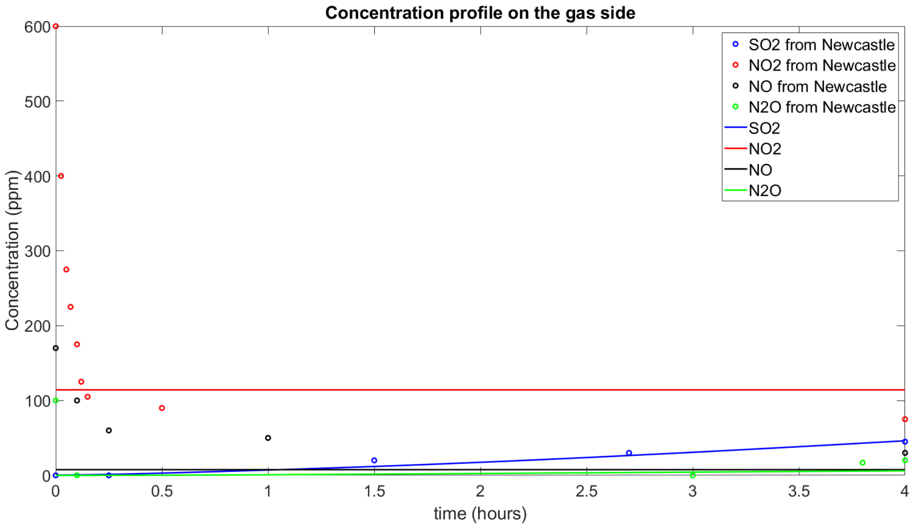

**Figure 6.5:** Comparison between the fitted version of the model and the results from the experimental work by Stanger et al.

The pH value decreases more in this fitted version of the model than in the original simulations since the volume of the liquid is smaller. It goes down to a pH value of approximately 1.9 instead of 3.5.

The $N_2O$ formation in this version of the model also seem to fit better with the results achieved in the experimental work. Although the formation of $N_2O$ starts earlier in the model and has a more steady growth, while the results from the experimental work show no formation until after three hours, except for the initial formation right at the start of their experiments. In relation to the $N_2O$ formation it is worthwhile to note that the pH at the end of this simulation was approximately 2. The bigger drop in pH compared to the original model which went down to a pH of approximately 3.5 is reasonable considering the volume of the liquid is considerably smaller in the fitted version.

Similarly the $NO$ and $NO_2$ fit better than in the original model. The trends are similar after the first 15-30 minutes. The $NO$ in the simulation is stalbe at a level slightly lower than they measured in the experimental work by Stanger et al. and the $NO_2$ is stable at a level slightly higher than what they measured.

It is possible that the discrepancy in the first 15-30 minutes between the results achieved from the experiments performed at Newcastle and the results from the simulations of the model could have to do with them measuring the dry interaction for 30 minutes and then seemingly immediately start the actual experiment.

### 6.1.4 Comparison of the dry interaction

In the dry interaction in the original experiments performed at the University of Newcastle, which can be seen in Figure 2.1 in the chapter about the results of the experimental work by Stanger et al., it should be noted that the final concentrations were approximately 600ppm $NO_2$, 500ppm $SO_2$ and 100ppm $NO$. The initial concentrations were 1000ppm $NO_x$ and 1000ppm $SO_x$. This means that approximately half the $SO_2$ and 300ppm $NO_x$ was consumed in the dry interaction in their experiments. It is however not specified what was formed instead.

To compare the dry interaction in their experiments the model was used to simulate a dry interaction as well. To simulate this the mass transfer removed so that only gas phase reactions could occur. The residence time was varied between simulations to compare with the results that were achieved during the experimental work by Stanger et al. The final composition in the gas phase is plotted against the residence time. The results of the simulations can be seen in Figure 6.6 below.

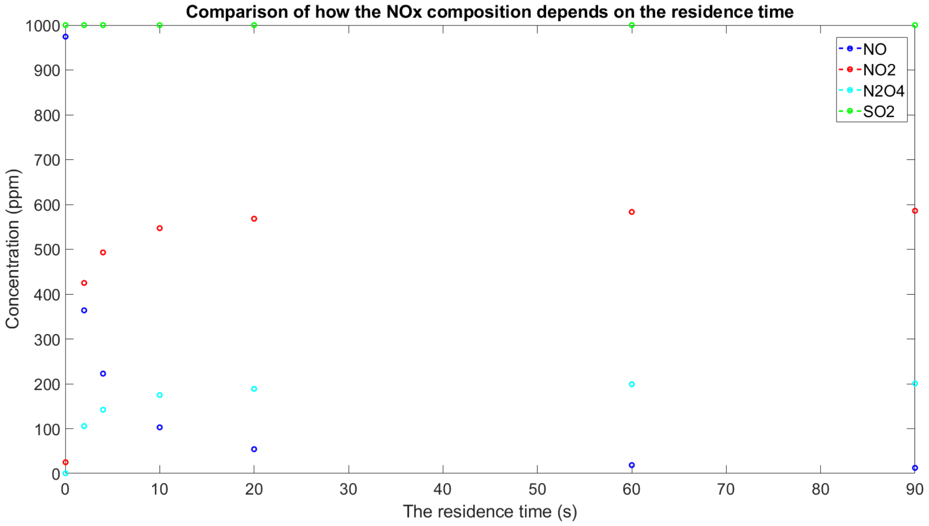

**Figure 6.6:** Analysis of the dry interaction that occurred before the gas phase was allowed to enter the liquid phase in the experiment at the University of Newcastle.

The $SO_2$ remains at 1000ppm in the model independent of the residence time. This happens since there is no reaction mechanism for $SO_2$ included in the gas phase chemistry in the model. The amount of $NO$ decreases as the residence time increases. The reason for this is that the longer the residence time is, the more time there is for the gas phase reactions to occur. For $NO$ it is mainly the oxidation to form $NO_2$, which is why the $NO_2$ inversely increases with the residence time. Similarly the amount of $N_2O_4$ also increases with the residence time since it requires $NO_2$ formation first to make subsequent $N_2O_4$ formation possible. Most of the reactions happen in the first 20 seconds and the system seems relatively stable after 60 seconds.

Since the $N_2O_4$ formation is not measured in the experimental work by Stanger et al. it can not be confirmed that it is formed there, but it seems likely that at least part of the $NO_x$ that is consumed in their gas phase is due to $N_2O_4$ formation.

The results of the simulations of the dry interaction in the model seem reasonable, but do not compare well with the results from the experimental work by Stanger et al. They believe there is interaction between $SO_2$ and $NO_x$ in the gas phase, which is not included in the model and can therefore not be compared.

## 6.2 Treatment alternatives for the liquid phase

In the following sections the alternatives for how to treat the remaining liquid phase will be evaluated. In order to evaluate the different alternatives changes will have to be made to the model to better describe the system of the treatment alternative in question.

The liquid phase that is used as basis for these simulations is the liquid phase that remains from the simulations of the experimental work by Stanger et al. This means that the data of the liquid phase was taken from the fitted version of the model.

### 6.2.1 Isolating the liquid phase

A basic overview of the system in the model when the liquid phase was kept isolated can be seen in Figure 6.7 below. It is a system consisting of a single batch reactor where the liquid phase is kept at constant pressure without the presence of a gas phase. This means that there is no mass transfer involved in this scenario. The pressure is kept at 1 atmosphere in the simulation, but the result would be the same for any other pressure as well. The pressure is however important for gas phase reactions, which are not excluded from this scenario. It does not have a direct impact on the liquid phase reactions. The initial composition of the liquid phase is the final composition of the liquid phase from the version of the model that is fitted to the results from the experimental work by Stanger et al.

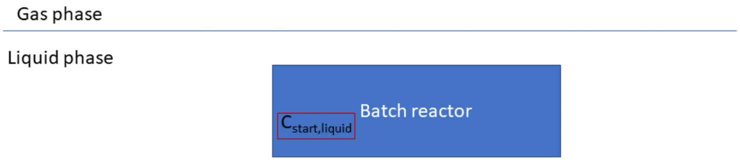

**Figure 6.7:** An overview of the model used to describe the system of the isolated liquid phase.

The reactions in the isolated liquid are very slow, as can be seen in Figure 6.9 and 6.8 below.

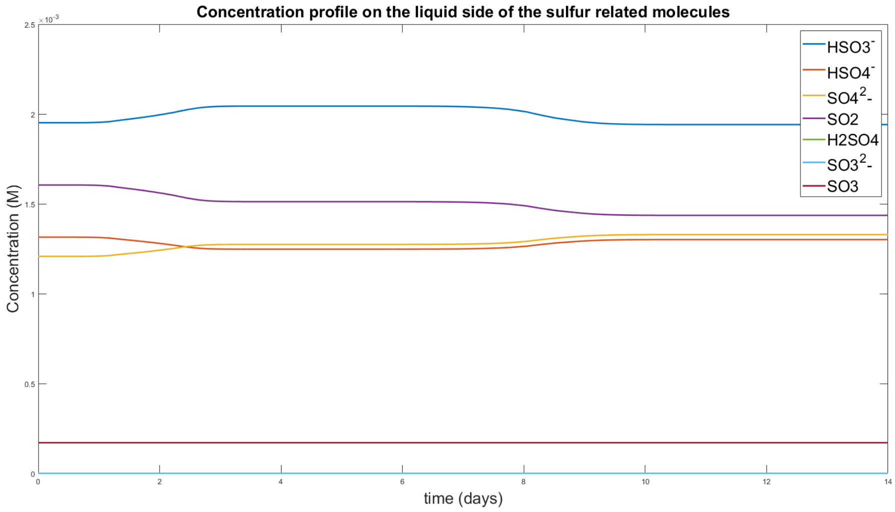

**Figure 6.8:** The concentration profile over the sulfur related molecules when the liquid phase is kept isolated under high pressure.

The $SO_x$ reactions happen much faster and seem to be relatively stable after approximately 3 days. These initial reactions are the consumption of $SO_2$ and $HSO_4^-$ to form $HSO_3^-$ and $SO_4^{2-}$ respectively. These are Reaction 3.10 and 3.11 in the theory chapter.

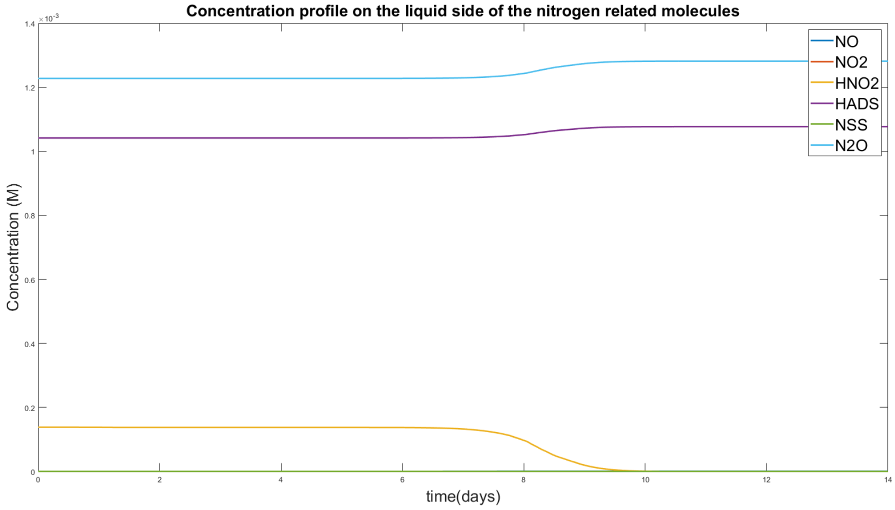

**Figure 6.9:** The concentration profile over the nitrogen related molecules when the liquid phase is kept isolated under high pressure.

While the $NO_x$ reactions require more time to get started. After approximately 5 days changes start to happen and visible changes in the graphs appear after approximately 8 days.

$NSS$ is formed from $HNO_2$ and $HSO_3^-$ and subsequently consumed in the formation of $NSS$. The following reactions where the $NSS$ in turn is consumed are very rapid which is why no $NSS$ formation can be seen in the graphs. There are two pathways in which the $NSS$ is consumed, one where $N_2O$ and $HSO_4^-$ are formed and one where $HADS$ is formed. All these three can be seen increasing around the 8 day mark, which is also where $HNO_2$ and $HSO_3^-$ are decreasing in the above mentioned reaction forming $NSS$. These reaction mechanisms can be seen in Reaction 3.14, 3.15 and 3.16 in the theory chapter. As the amount of $HSO_4^-$ increases it also reacts and forms $SO_4^{2-}$ through Reaction 3.10. The reactions continue until the $HNO_2$ is completely consumed, as can be seen in Figure 6.9. While it can be seen in Figure 6.8 that all the $HSO_3^-$ is not consumed.

### 6.2.2 Releasing the liquid phase into a waste water pound

A basic overview for the system in the model that is used to describe the scenario of releasing the liquid phase into a waste water pound can be seen in Figure 6.10 below. The system is modeled as two batch reactors, one for the liquid phase and one for the gas phase. The pH value of the system is kept constant at a pH of 7 as the volume of the released liquid is very small compared to the volume of a waste water pound. The volume of the gas phase is much larger than the volume of the liquid as the air surrounding has a significantly larger volume than the waste water pound itself. The inter facial area per volume is worse in this scenario than it is for a bubble column and the inter facial area is therefore decreased to account for this.

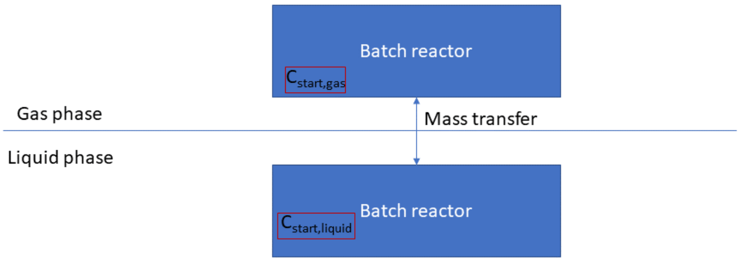

**Figure 6.10:** An overview of the model used to describe the system for releasing the liquid into a waste water pound.

#### 6.2.2.1 Immediate release of the liquid phase into a waste water pound

The result of immediately releasing the liquid phase into a waste water pound with a pH of 7 can be seen in Figure 6.11, 6.12 and 6.13 below. The waste water pound starts to release $N_2O$ into the atmosphere almost instantly, but at a very low rate and it is not until around 1.5 days that the release increases in pace. More relevant than the ppm of $N_2O$ emissions, the $N_2O$ consists of 39.2% of the total amount of nitrogen that was released into the waste water pound.

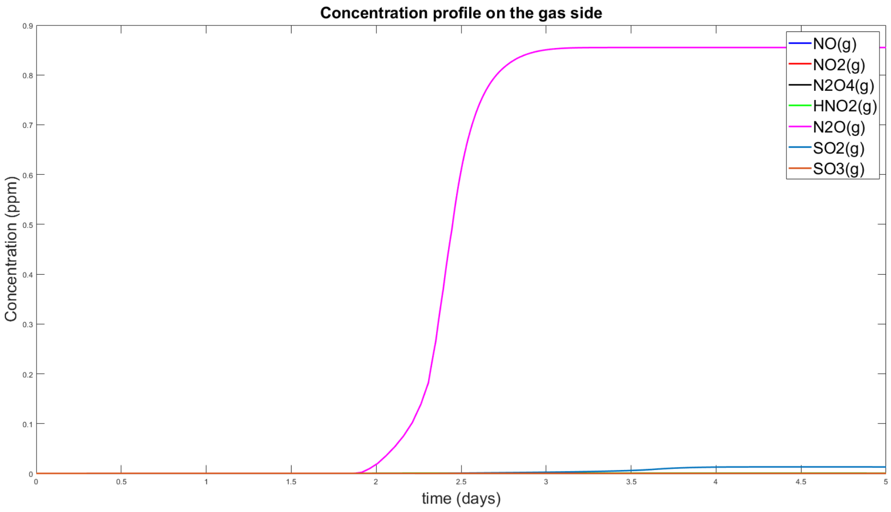

**Figure 6.11:** The concentration profile of the gases that enter the air due to the immediate release of the liquid phase into the waste water pound.

It can be seen that most of the reactions in the liquid phase start relatively quickly and the liquid is seemingly stable after 1.5 days. The $HNO_2$ reacts and forms $NO_2^-$. While the $SO_2$ reacts and forms $HSO_3^-$, which in turn forms $SO_3^{2-}$. These reaction pathways can be seen clearly in Figure 6.12 below.

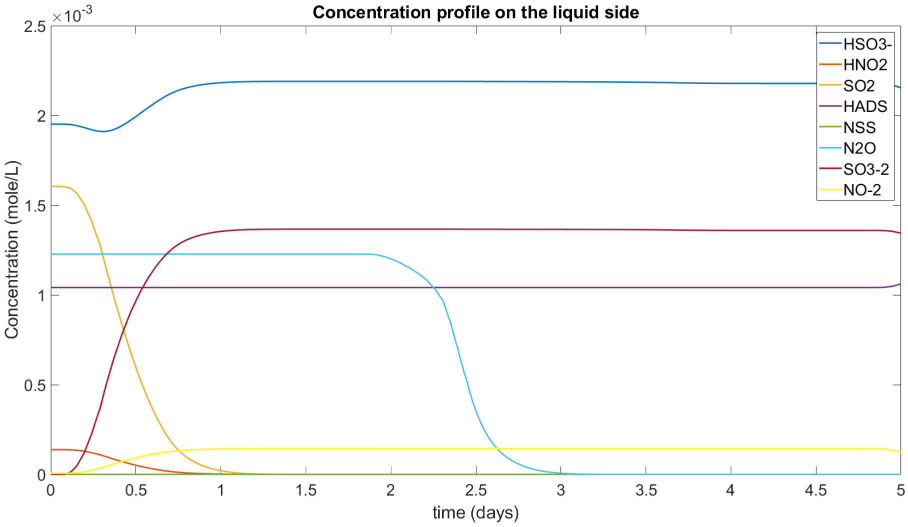

**Figure 6.12:** The concentration profile in the water when the liquid phase is released into a waste water pound.

While it looks like everything is stable except $N_2O$ in the period after 1.5 days in Figure 6.12 above, it can be seen in Figure 6.13 below that it is not the case. It can be seen that once $HNO_2$ is mostly consumed and stable and $HNO_3$ is completely consumed both $NO$ and $NO_2$ in turn are consumed. The reactions where $NO$ and $NO_2$ are consumed will form additional $HNO_2$ and possibly $HNO_3$ as well. This additional formation does not show in the graph which means that it must be quickly consumed in another reaction. Considering the amount of $N_2O$ that is released into the atmosphere in this time period it is likely that there is newly formed $HNO_2$ which reacts with $HSO_3^-$ to form $NSS$.

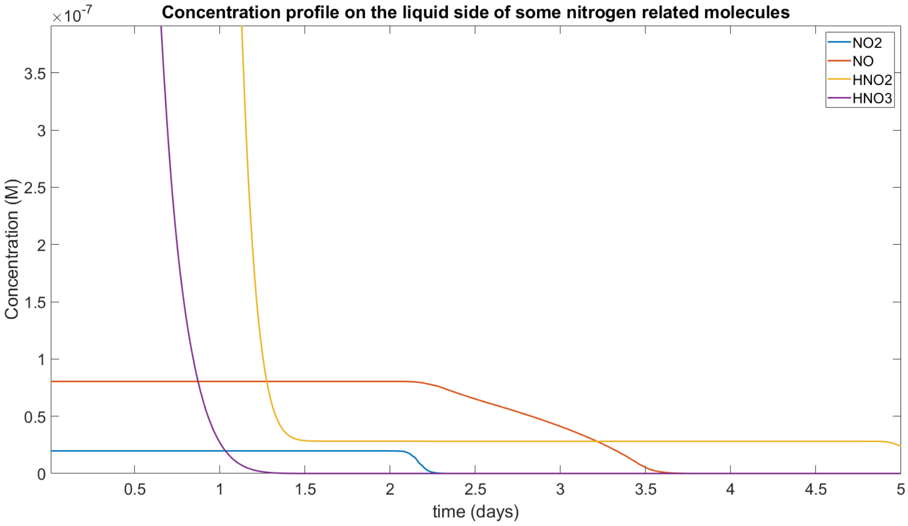

**Figure 6.13:** The concentration profile in the water when the liquid phase is released into a waste water pound.

In Figure 6.14 below it can be seen that there is a continuous consumption of $HSO_3^-$

in this time frame as well which makes it reasonable to assume that $NSS$ is formed in this time frame, which also causes the $N_2O$ release into the atmosphere that can be seen in Figure 6.11 above.

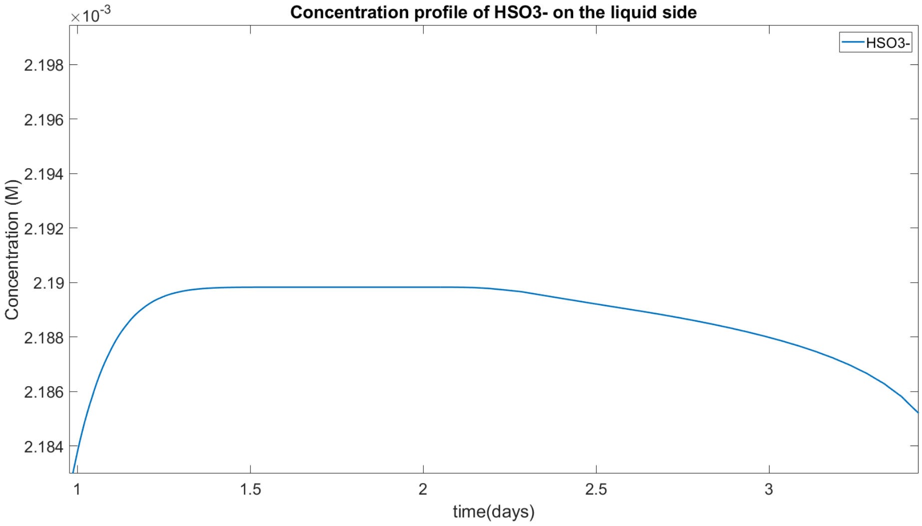

**Figure 6.14:** The concentration profile in the water when the liquid phase is released into a waste water pound.

#### 6.2.2.2 Release of the liquid phase into a waste water pound after having kept it isolated

When keeping the liquid phase isolated the composition changes for some time until it becomes stable. This could be seen in figure 6.9 and 6.8 above. In order to evaluate the impact of the isolation as an alternative to releasing the liquid immediately it was simulated releasing the liquid with the composition that it achieved after being kept isolated. This can be seen in Figure 6.15 and 6.16 below.

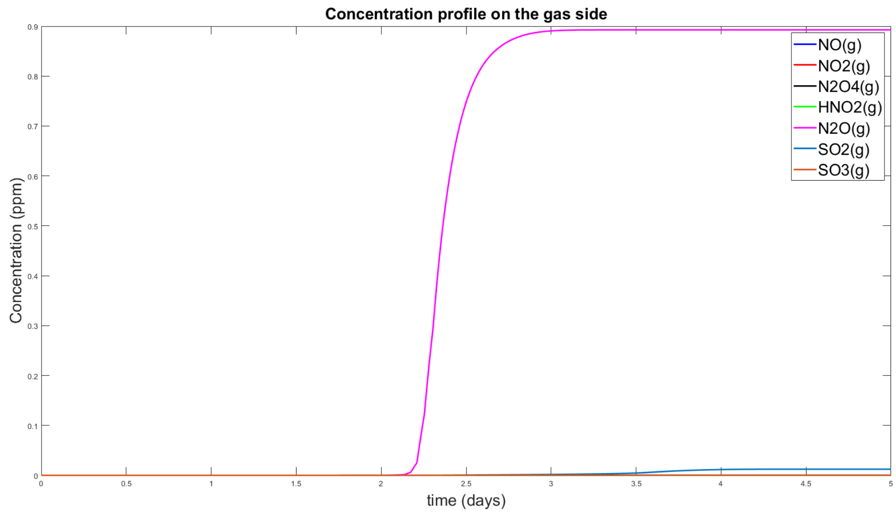

**Figure 6.15:** The concentration profile for the gas phase composition that leaves the waste water pound when the isolated liquid phase is released there.

The amount of $N_2O$ that is released into the atmosphere is slightly larger in this scenario. The amount in the graph goes up to almost 0.9 ppm, but more importantly the release of $N_2O$ into the atmosphere consists of 41.15% of all the nitrogen that was released into the waste water pound.

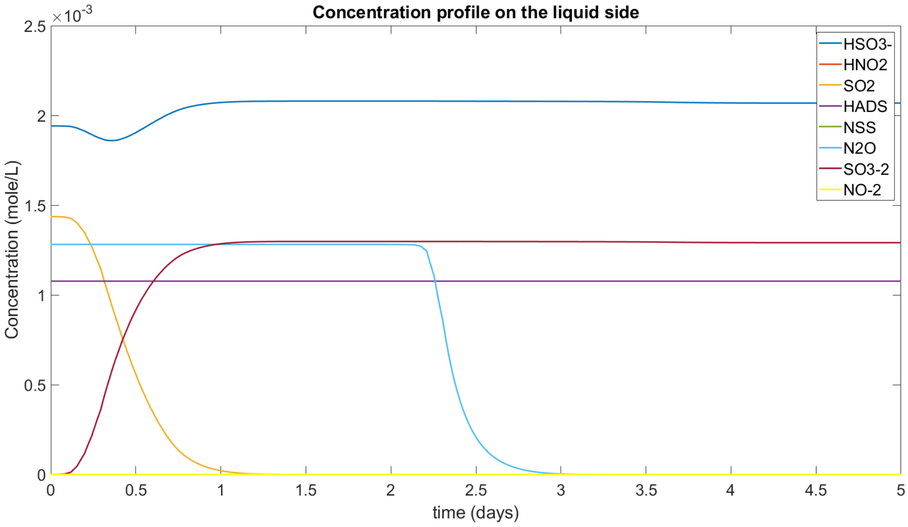

**Figure 6.16:** The concentration profile for the liquid phase composition that leaves the waste water pound when the isolated liquid phase is released there.

The trends that can be seen in Figure 6.16 above are very similar to those from Figure 6.12 above. A major difference is that there is no $HNO_2$ present when the liquid is released into the waste water pound in this scenario as it has already been consumed during the isolation. The amount of $N_2O$ is also a slight bit higher at the point of release since additional $N_2O$ was formed during the isolation, this is likely the main reason to why there is a higher amount of $N_2O$ emissions in this scenario compared to the scenario where the liquid is immediately released.

#### 6.2.2.3 Release of the liquid phase into a waste water pound with a pH of 4

If there would be a continuous release of the liquid phase that remains from the reactor without any previous treatment, then it would over time lower the pH level of the waste water pound. It is therefore relevant to simulate what would happen in a scenario where the waste water pound's pH levels would be lowered. This can be seen in Figure 6.17 and 6.18 below. There is a similar, but slightly higher, amount of $N_2O$ released in this scenario which consists of approximately 39.5% of the total nitrogen added to the waste water pound through the release of the liquid. There is also high increase in the release of $SO_2$ into the atmosphere in this scenario.

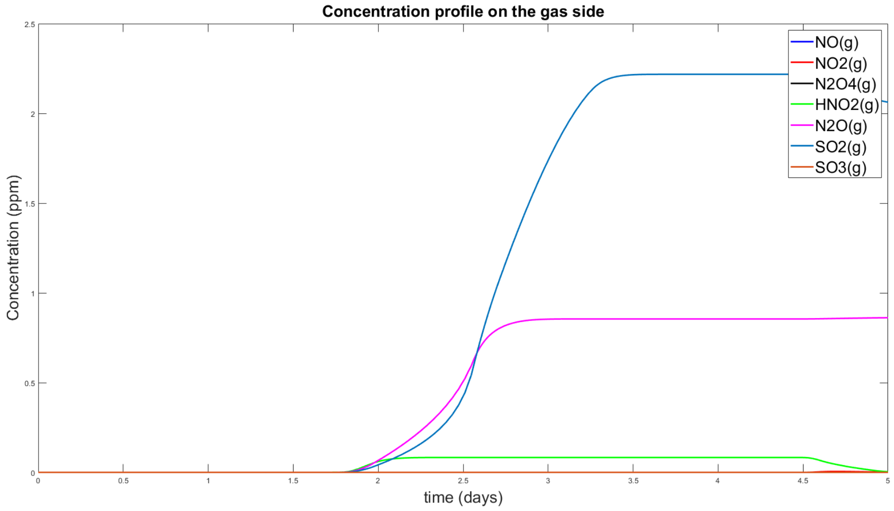

**Figure 6.17:** The concentration profile of the gases that enter the air due to the immediate release of the liquid phase into a waste water pound with a pH of 4.

There are some differences in the chemistry regarding $SO_2$, $HSO_3^-$ and $SO_3^{2-}$ when the pH is lowered to 4. The reaction from $HSO_3^-$ to $SO_3^{2-}$ does not seem to occur in this scenario and therefore there is no increase of $SO_3^{2-}$, instead the initial increase of $HSO_3^-$ is larger. When the release of $SO_2$ into the atmosphere starts it is the $HSO_3^-$ on the liquid side that decreases as it reacts to form $SO_2$ in the liquid phase which subsequently transfers from the liquid phase into the gas phase.

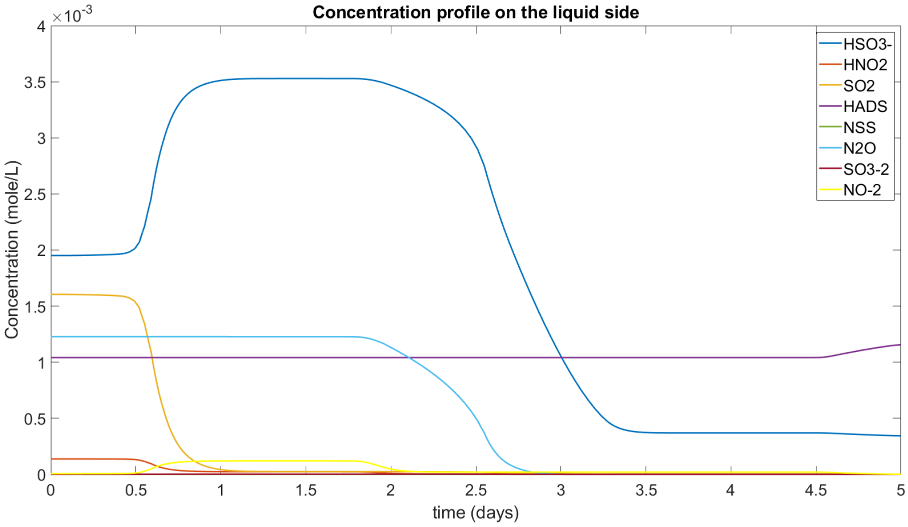

**Figure 6.18:** The concentration profile when the liquid phase entered a waste water pound with a pH of 4.

### 6.2.3 Sensitivity analysis of the inter facial area

There is uncertainty regarding how accurate the inter facial area in the model is at describing the inter facial area for mass transfer between the water in the waste water pound and the air above it. The importance of this value is compared by decreasing the value of the inter facial area in the model and evaluate the impact it has on how much $N_2O$ that is released into the air. The original value of the inter facial area is the calculated value for the reactor that was used for the simulations of the experimental work by Stanger et al. It is reasonable to assume that the real value for a waste water pound would be smaller as the inter facial area in a bubble column is relatively high. The results can be seen in Figure 6.19 below.

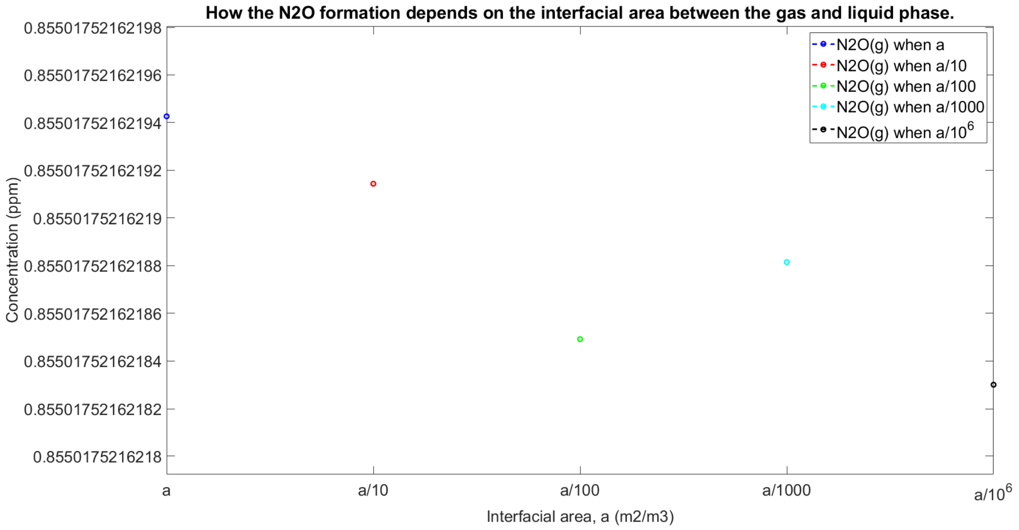

**Figure 6.19:** A sensitivity analysis on how much impact the inter facial area for mass transfer between the waste water pound and the surrounding air has on the mass transfer of $N_2O$ into the air.

The difference in the amount of $N_2O$ that is emitted into the air between the different inter facial areas is very small. This means that changing this parameter does not make a significant difference on the results for releasing the liquid phase into a waste water pound. This is likely due to the reactions in the liquid phase being relatively slow compared to the mass transfer of $N_2O$ into the gas phase, air.

### 6.2.4 Sensitivity analysis of the volume ratio between the gas phase and the liquid phase

There is also uncertainty regarding the volumes to use for the gas phase, the air, and the liquid phase, the water, when simulating the release of the liquid into a waste water pound. Therefore it was important to also perform a sensitivity analysis on how this ratio impacts the system and most importantly the emissions of $N_2O$ into the air.

The ppm of $N_2O$ released into the gas phase is shown in Figure 6.20 below. It can be seen that the amount of ppm decreases as the ratio increases, this is reasonable since the ratio is changed by increasing the volume of the gas phase.

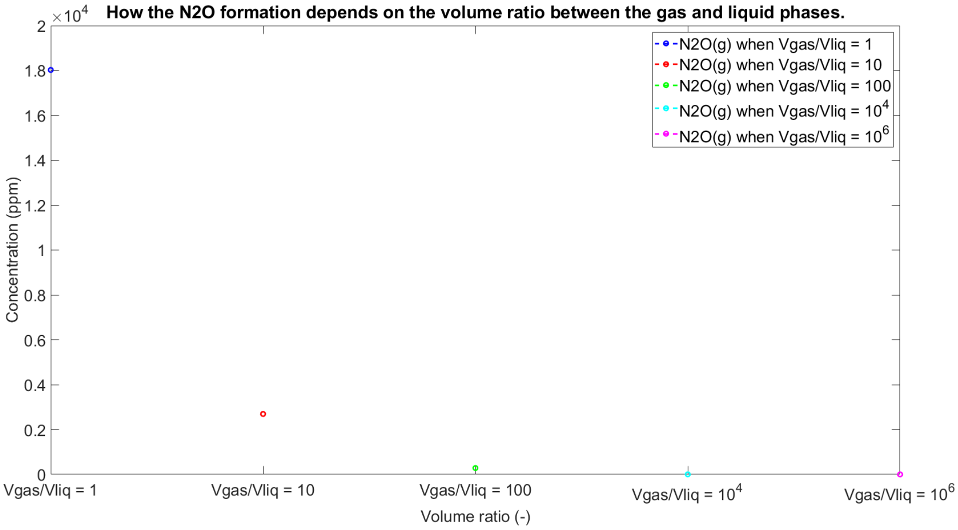

**Figure 6.20:** A sensitivity analysis on how much impact the ratio of volume between the gas phase and liquid phase have on the mass transfer between the waste water pound and the surrounding air has on the mass transfer of $N_2O$ into the air.

It can be seen in Table 6.2.4 below how the actual share of nitrogen released into the waste water pound that gets released as $N_2O$ emission depends on the ratio between the volumes of the gas phase and the liquid phase.

| Vgas/Vliq ratio | Percentage of nitrogen molecules from the liquid phase emitted into the air as $N_2O$ |
|---|---|
| 1 | 24.8 % |
| 10 | 37.0 % |
| 100 | 39.0 % |
| $10^4$ | 39.2 % |
| $10^6$ | 39.2 % |

**Table 6.1:** An overview of the percentage of nitrogen molecules from the liquid phase that gets emitted into the air as $N_2O$ depending on the ratio between the volume of the gas phase and liquid phase.

The important part is that once the volume of the gas phase is sufficiently large the share of nitrogen molecules that gets released into the air as $N_2O$ emissions stabilizes. Therefore it does not play a major role on the results as long as the ratio is significantly large, which is a reasonable assumption to make as the air above the waste water pound should be of a significantly larger volume than the volume of the waste water pound itself.

### 6.2.5 Global warming potential

Greenhouse gases, such as $CO_2$ and $N_2O$, contribute to global warming by slowing the rate at which the energy leaves the earth. Global warming potential (GWP) is a method of comparing the impact different gases have on the global warming. $CO_2$ is the reference gas and the others are measured as how much impact they have in comparison to $CO_2$. $N_2O$ has a GWP of 265-298 times that of $CO_2$, which makes it a very powerful greenhouse gas [8].

Out of the 1000 ppm $NO_x$ that entered the reactor for simultaneous $NO_x$ and $SO_x$ removal in the fitted model approximately 140 ppm remained in the gas phase. Which means that approximately 860 ppm got absorbed into the liquid phase. Of the absorbed 860 ppm in the liquid phase approximately 40% formed $N_2O$ when released into the waste water pound. This is equivalent to having approximately 344 ppm $N_2O$ or 10% $CO_2$ in the flue gas stream.

# 7

# Conclusion

In this thesis the experimental work by Stanger et al. is compared through modelling with the detailed reaction mechanism by Ajdari et al. on simultaneous $NO_x$ and $SO_x$ removal from the flue gases for a pressurized oxy-fuel combustion system. The parameters in the model were adjusted to fit with the results that were achieved from the experimental work in order to validate the model. By decreasing the volume of the liquid and the mass transfer coefficients in the model a satisfactory fit was found. Mainly the $SO_2$ absorption in the model match the results from the experimental work and the $N_2O$ have a similar trend although the $N_2O$ formation is slightly lower in the model. The lower formation is most likely due to a lower level of $NO_2$ absorption in the model. The fitted model was then used to obtain data on the liquid phase, which was not measured in the experimental work by Stanger et al., to evaluate different treatment alternatives for the liquid phase that remains.

In the scenario where the liquid phase is immediately released into a waste water pound there is an unwanted release of $N_2O$ which consists of approximately 39.2% of the nitrogen that was in the liquid phase. This is not a very large amount in this case, but it is a very significant share of the nitrogen which forms $N_2O$ and subsequently gets released into the atmosphere. If the process was to be up scaled then it would become considerable $N_2O$ emissions.

Isolation from the atmosphere of the liquid leads to an increase in $N_2O$ formation both during the isolation and if the isolated liquid was to be released to an open atmosphere at a later stage. The unwanted release of $N_2O$ when the liquid phase had been isolated first was approximately 41.15% of the nitrogen that was in the liquid phase. This is an increase of almost 2% of the nitrogen compared to when the liquid was immediately released.

If liquid were to be released into the same waste water pound over an extended period of time it would lead to the pH value of the waste water pound decreasing since the pH value of the liquid is low, approximately 1.9. Lower pH value favors the reaction pathway that leads to $N_2O$ formation. In the scenario of releasing the liquid phase into a waste water pound with a pH value of 4 the $N_2O$ released into the air would consist of approximately 39.5% of the nitrogen molecules. This is an increase of 0.3% compared to when the pH value of the waste water pound was constant at 7. It would therefore be preferable to increase the pH value of the liquid before releasing it or to use a buffer solution in the waste water pound to keep the pH level stable.

## 7.1 Further work

There are uncertainties regarding the mass transfer mechanism in the model. Further work on a more detailed mass transfer mechanism could improve the understanding of the system. Possibly in combination with more experimental work.

Potentially the liquid phase could be released into a waste water pound together with a buffer to keep the pH value stable. This would need to further work to evaluate its impact.

# Bibliography

[1] Ajdari, S., Normann, F., Andersson, K., Johnsson, F. (2015) *Modeling the nitrogen and sulfur chemistry in pressurized flue gas systems.* Department of energy and environment, Chalmers university of technology, Gothenburg, Sweden.

[2] Stanger, R., Wall, T. (2019) *Laboratory measurements: N2O formation and co-removal of NOx and SOx in oxyfuel flue gas compression.* Chemical Engineering, University of Newcastle, Newcastle, Australia.

[3] Welty, J.R., Wicks, C.E., Wilson, R.E., Rorrer, G.L. Fundamentals of momentum, heat, and mass transfer. Fifth ed. 2007: John Wiley & Sons.

[4] Seader, J.D., Henley, E. J., Separation process principles. Second ed. 2006: John Wiley & Sons.

[5] Sridhar, T., Potter, O.E. (1979) *Gas holdup and bubble diameters in pressurized gas-liquid stirred vessels.* Department of chemical engineering, Monash university, Clayton, Victoria, Australia.

[6] Kraume, M., Zehner, P. (2005) *Bubble columns.* BASF Aktiengellschaft, Federal Republic of Germany.

[7] Levenspiel, O. Chemical reaction engineering. Third ed. 1999: John Wiley & Sons.

[8] United States Environmental Protection Agency, *"Understanding Global Warming Potentials,"* 2019. [Online]. Available: https://www.epa.gov/ghgemissions/understanding-global-warming-potentials